water

MDPI

Article

Nutrients, Organic Matter, and Trace Elements in Lake Gusinoe (Transbaikalia)

Zinaida Ivanovna Khazheeva *, Aleksey Maksimovich Plyusnin, Olga Konstantinovna Smirnova, Elena Georgievna Peryazeva, Seseg Sergeevna Sanzhanova, Dashima Ivanovna Zhambalova, Svetlana Gennadievna Doroshkevich and Viktoriya Valerievna Dabaeva

Geological Institute of SB RAS, 670047 Ulan-Ude, Russia; plyusnin@ginst.ru (A.M.P.); meta@ginst.ru (O.K.S.); peryazeva75@mail.ru (E.G.P.); sanzhanova7@rambler.ru (S.S.S.); dachima@mail.ru (D.I.Z.); gin@ginst.ru (S.G.D.); dv.viktoriya@mail.ru (V.V.D.)

* Correspondence: zina.zkhazh@mail.ru; Tel.: +7-90-2162-2534

Abstract: Lake Gusinoe is the second largest freshwater lake in Transbaikalia. Lakes serve as a source for drinking water, irrigation, and as a water source for the electricity, aquatic production, and tourism industry. Currently variations of content nutrients and organic matter differ in different areas of the lake. The content of total nitrogen, phosphorus, organic matter, and dissolved oxygen are distinguished more than 1.2–2.0 times. In accordance with the behavior of elements in the water, three groups of elements can be distinguished. The first group of elements, including Li, Ga, Ge, As, Rb, Sr, Mo, Cd, W, and U, were directly correlated with variations of major elements. The first group of elements showed decreasing concentrations with an increasing amount of total dissolved salt (TDS). The second group of elements, including Fe, Y, Nb, Th, and REE, were correlated oppositely with variations of TDS. The behavior of the third group of elements, including Mn, Zn, Ni, Cu, and Pb, decoupled with TDS. The value of the Eu anomaly was positively correlated with TDS. The water of Lake Gusinoe was extremely enriched by W, Mo, V, U, Li, Sr, and Ga; moderately by Ni, Cu, Ge, As, Rb, Cd, and Pb; and minimally by Al, Cr, Mn, Fe, Co, Zn, Y, Th, and REE.

Keywords: fresh water; nutrients; organic matter; enrichment trace element

check for updates

Citation: Khazheeva, Z.I.; Plyusnin, A.M.; Smirnova, O.K.; Peryazeva, E.G.; Sanzhanova, S.S.; Zhambalova, D.I.; Doroshkevich, S.G.; Dabaeva, V.V. Nutrients, Organic Matter, and Trace Elements in Lake Gusinoe (Transbaikalia). *Water* **2021**, *13*, 2958. https://doi.org/10.3390/w13212958

Academic Editor: Rinat M. Manasypov

Received: 31 August 2021
Accepted: 18 October 2021
Published: 20 October 2021

1. Introduction

Lake Gusinoe (51.2° N, 106.5° E) is a freshwater lake in the southwest of Transbaikalia, the second largest body of water after Lake Baikal. It has a watershed area of about 924 km^2; a maximum width and depth of 8.5 km and 25–30 m; a water surface area of 164 km^2; a volume of water of 2.4 km^3; and a shoreline length of 25 km. The tributaries of the lake are represented by 72 small rivers and their total length is 312 km. The river Tsagan-Gol (85% of the inflow) is in the southwest, river Zagustai is in the northeast, smaller rivers flow from the Khambin Ridge into the lake. The streams of the Monostoi Ridge are insignificant and seasonal. Part of the lake is fed by underground sources. The reservoir has a single flow out at the southern end of the lake. The Bayan-Gol River flows out at the left tributary of the Selenga River. At the northeast, the city Gusinoozersk is located on the slopes of Monostoi and the Zagustai valley adjoins the lake. The Tamchinskaya flatplain is southwest of the reservoir (Figure 1).

The region has a severely continental climate with negative average annual temperatures (−2 to −3 °C), a short frost-free period (95–100 days), and a relatively small amount of precipitation (200–300 mm). The negative average monthly air temperature continues for six months; therefore, the lakes freeze to significant depths of 1.2–1.4 m. The region has a severely continental climate with negative average annual temperatures (−2 to −3 °C), a short frost-free period (95–100 days), and a relatively small amount of precipitation (200–300 mm). The negative average monthly air temperature continues for six months; therefore, the lakes freeze to significant depths of 1.2–1.4 m.

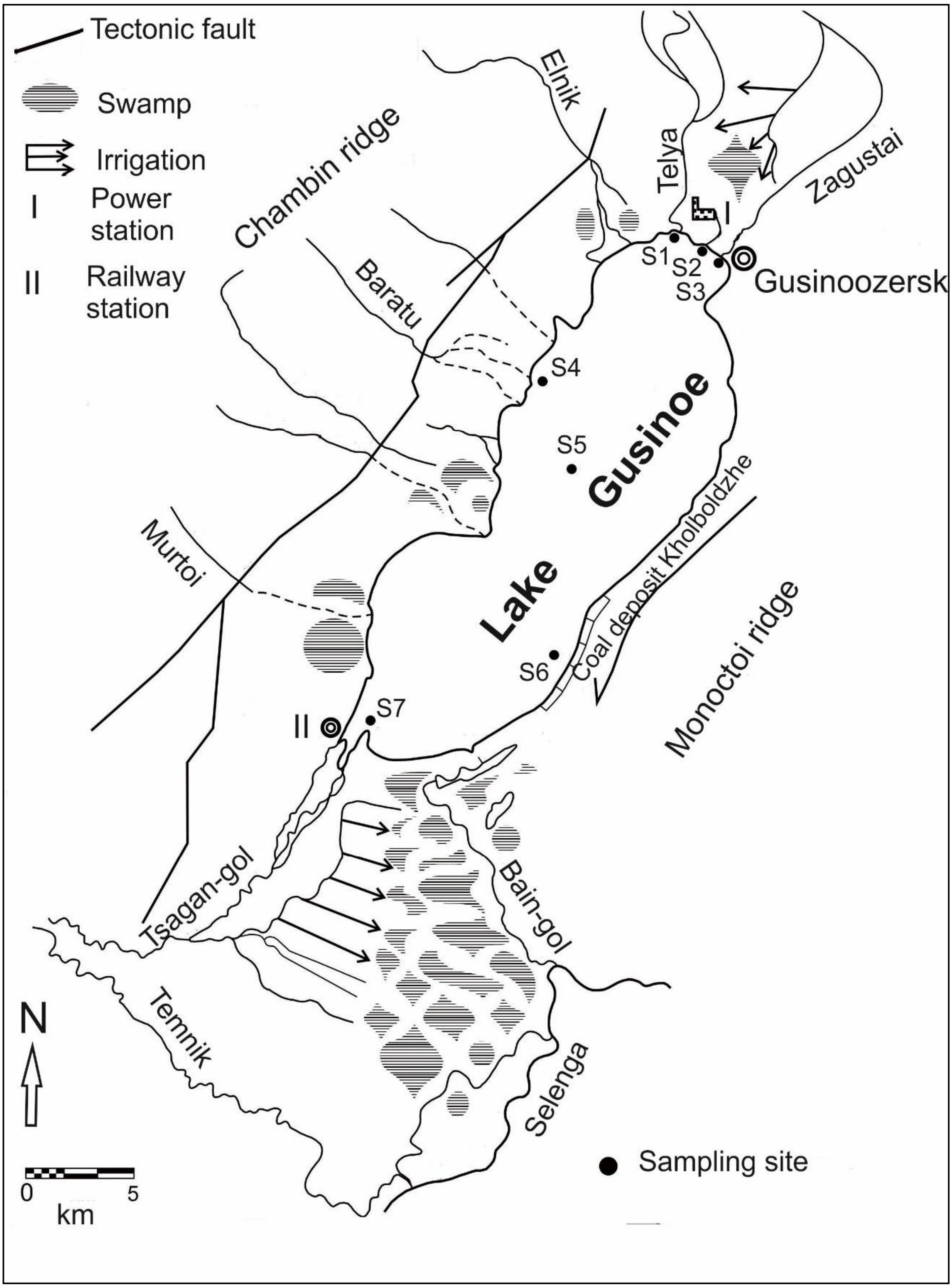

Figure 1. Sampling site at Lake Gusinoe.

A specific geologic feature of the study area is the presence of late Mesozoic carbonatites on the northwestern flanks of the Gusinoe Ozero–Orongoi and Ivolga depressions [4]. Carbonatites are present as dikes, manto deposits, and steeply dipping breccias; they are associated with alkaline high-K rocks and are referred to as both REE (Arshan and Yuzhnoe (southern) occurrences) and essentially Ba–Sr (Khalyuta and Oshurkovo) types.

The carbonatites are enriched in sulfate sulfur. The content of their sulfate minerals often reach 20–30%. The total content of SO_3 is 2.85–13.60% in the Khalyuta carbonatite field, 0.68–8.82% in the Oshurkovo field, 1.42–10.82% in the Arshan field, and 0.83–3.08% in the Yuzhnoe field. At this location, sodium and potassium sulfates well soluble in water are the most widespread sulfate minerals [5]. Therefore, carbonatites of the above occurrences have surficial caverns resulting from the leaching of well-soluble alkali metal sulfates. As known from the report by G.S. Ripp, alkali metal sulfates are readily extracted from carbonatites by leaching with distilled water [6].

The Gusinoe Ozero–Orongoi depression is filled with continental sediments including rocks of different lithologies from coarse-pebble conglomerates and inequigranular sandstones to silts and coals of the Lower Cretaceous Gusinoe Ozero Group [2,3]. The sediments of this group are subdivided into four formations (from bottom to top): Murtoi, Ubukun, Selenga, and Kholboldzhe. All the formations conformably rest upon each other. The Murtoi formation lays over the Ichetui Formation volcanics.

Three aquifer systems have been recognized within the depression: (1) Firstly, quaternary sediments with pore–stratal groundwater have been found and pebbles, sands, and sandy loams are water-bearing rocks. These waters usually occur at a depth of 2–4 m, seldom reaching a depth of 22 m. They are fed by atmospheric precipitation, surface waters, groundwater of coal-bearing strata, and crystalline-rock water. The waters of this complex are mostly fresh calcium–magnesium bicarbonates; (2) Secondly, sediments of the Gusinoe Ozero group with stratal and formation–fracture waters have been found. The waters in the rocks of the Murtoi and Ubukun formations are sodium bicarbonates with $TDS \leq 0.5\ g{\cdot}L^{-1}$. The rocks of the Selenga formation enclose calcium–sodium sulfate–bicarbonate waters with $TDS \leq 2.2\ g{\cdot}L^{-1}$. This aquifer system is fed by atmospheric precipitation and fracture waters of crystal-line rocks; (3) Thirdly, the crystalline basement is formed by Paleozoic and Mesozoic granitoids, as well as by the Triassic (Mesozoic) effusive rock complex. Fault zones are characterized by the highest water abundance, permeability, and porosity. The spring water of lower Cretaceous sediments contain up to SO_4^{2-} 693 $mg{\cdot}L^{-1}$ and up to Cl^- 212 $mg{\cdot}L^{-1}$ [6].

The banks are treeless and have steppes, and only in the northwest at the mouth of the Yelnik stream, there is a small massif of coniferous forest with an area of about 1 km^2. The western, northern, and partly southern coasts of Lake Gusinoe are swampy, especially at the mouths of rivers which streams flow into. The coastal bottom is muddy and covered with aquatic vegetation. For the most part, the eastern coast for 20 km forms a narrow sandy beach with clear water, suitable for recreational purposes. The bottom of the lake consists of two parts, separated by the crystalline uplifting that extends from the Kholboldzhe coal-bearing syncline at the eastern part to the railway station at the southern part of the lake [2,3].

The Gusinoozersky industrial hub is one of the largest in Buryatia and includes coal mining, energy producing, and transport enterprises, most of which are located in the northern and northeastern shores of the lake. Along the northeastern shore of the lake is the Kholboldzhe coal mining factory and in the southwestern part of the lake, there is a large railway station and a locomotive depot. Warm waters from the Gusinoozerskaya hydroelectric power station, industrial storm sewerage, and ash dumps flow into the lake. One fourth of the lake's water resources is used to cool the power station units. The sewage treatment facilities of the city Gusinoozersk are a stable source of pollution to the lake. The treatment plant uses mechanical and biological methods after water is chlorinated and discharged into the lake. The lake water is used for drinking water, irrigation, recreation, electricity generation, for washing and cleaning, and for the fish culture. The mixing of sewage and waste materials into the lake, as well as the decomposition of vegetation directly result in lake pollution.

In recent years, extensive research has been carried out on the anthropogenic use and subsequent changes of lakes in different regions [7–10]. Lake Onego, located in the northwest of the Russian Federation, is the second largest freshwater lake in Europe. Lake

Onego represents an important freshwater resource used to supply cities, residential areas, and large industrial centers, but suffers from industrial, urban, and agricultural pollution. The lake connects to the White Sea through the White Sea–Baltic canal and connects to the Caspian and Black Seas through the Volga–Baltic waterway and Volga River, thus representing a major transportation route. Eutrophication and chemical pollution derive from point sources [11]. The results of comprehensive hydro–physical, hydrobiological, and hydro–chemical studies are summarized by several authors [12–16].

The expansive and economically important North American Great Lakes are subjected to multiple stressors and understanding their responses to those stresses is important for understanding system-wide ecological controls. Phytoplankton production is an important factor in determining both ecosystem stability and the provision of ecosystem goods and services. These changes indicate that the lakes have undergone gradual oligotrophication coincidence with and anticipated by nutrient management implementation [17–26].

Lake Baikal is located in eastern Siberia in the center of a vast mountain region. Even though the lake is regarded as a unique and pristine ecosystem, there are existing sources of anthropogenic pollution to the lake. The concentrations of the potentially toxic trace elements As, Cd, Pb, Hg, and Se were analyzed in water, plankton, invertebrates, and fish from riverine and pelagic-influenced sites in Lake Baikal. Concentrations of Cd, Hg, Pb, and Se in Lake Baikal water and biota were low, while concentrations of As were similar or slightly higher compared to that in other freshwater ecosystems [27].

In recent years, regarding the rapid development of the local economy in the Siberia of Russia and the subsequent intensive uses of water resources, surface water pollution has become increasingly serious, restricting the sustainable development of the local economies. Anthropogenic activities result in a significantly decreased surface water quality in the aquatic systems in watersheds.

The goal of this paper is to determine changes in the aquatic ecosystem of Lake Gusinoe, as impacted by anthropogenic influences of varying intensities.

2. Materials and Methods

In sampling the water, suspended materials were examined monthly from March to October for three years during 2016–2018. The sampling sites are shown in Figure 1, while their list and locations are summarized in Table 1.

Table 1. Sampling site and their location within Lake Gusinoe.

Sample Site	Location and Anthropogenic Impact
S1	The inflow of the Telya river. Production areas of the electricity power station.
S2	The inflow warming water of the electricity power station.
S3	Wastewater after treatment (WWTP) from the city of Gusinoozersk inflows in Zagustai River.
S4	Agriculture and animal husbandry of the rural population.
S5	The center of the lake, involved in fishing.
S6	Mine water of the coal-bearing Cholboldze deposit.
S7	The inflow of the Tsagan-gol River that flows out from the Temnik mountain river, resting in natural conditions. The railway station is at a distance of 0.8–1.3 km.

Water samples were collected by 3 L polypropylene bottles at 0.5 and 2.5 m below the surface at the 7 sampling sites. The water samples were immediately preserved at 4 °C in darkness and analyzed within 48 h.

The temperature T °C, pH, and DO were determined directly at each sampling site. The pH was measured by the pH meter Beckman Model F8 253 (Beckman, Pasadena, CA, USA), the DO by a YSI oxygen meter, Model 57 (YSI, Yellow Springs, OH, USA), and the temperature by the RST 07953 (Sweden-China).

The filter, which was situated through a 0.45 µm pore size, was used for the determination of dissolved inorganic nitrogen NH_4-N ($mg \cdot L^{-1}$) and NO_2-N + NO_3-N ($mg \cdot L^{-1}$), as well as for dissolved inorganic phosphate PO_4^--P ($mg \cdot L^{-1}$), which were determined by standard methods and measured using spectrophotometric determination NH_4-N (λ = 630 nm), NO_2-N$^-$ (λ = 543 nm), TN (λ = 207 nm), and PO_4-P (λ = 882 nm). Total nitrogen TN and phosphorus TP were determined in unfiltered samples. The concentration of organic phosphorus P_{org}, Norg, was determined from the difference between the concentrations of the total phosphorus and the mineral phosphorus. The chemical oxygen demand, COD (COD_{Cr}), and biological oxygen demand, BOD_5, were determined in unfiltered samples [28–30].

The trace and REE elements were determined by the ICP-MS method on a double-focusing mass spectrometer and an ELEMENT XR cross-flow atomizer (Thermo Finnigan, Bremen, Germany) in the Lab of Physical Methods of Analysis at the Geological Institute, Siberian Branch, Russian Academy of Sciences. The index for the water pollution (WPI) was calculated as follows.

$$\mathrm{WPI} = \left(\sum_{i=1}^{6} C_i / MPC_i\right)/6 \tag{1}$$

where C_i corresponds to the concentration of the water parameter and MPC_i corresponds to the maximum permissible concentration (Table 2).

Table 2. Maximum permissible concentration of each parameter as regulated by hygienic norms, specifically HN 2.15.1315-03 [31].

Parameter	Unit	Maximum Permissible Concentration
DO	$mgO_2 \cdot L^{-1}$	>6
BOD_5	$mgO_2 \cdot L^{-1}$	3
NH_4-N	$mgN \cdot L^{-1}$	0.39
NO_3-N	$mgN \cdot L^{-1}$	9.0
PO_4-P	$mg \cdot L^{-1}$	0.66
Fe	$mg \cdot L^{-1}$	0.3

3. Results and Discussion

In [32], it was annually shown that at sites S1–S6, the TDS (total dissolved salt) of the lake water varied from 118 to 343 $mg \cdot L^{-1}$; the content of anions was determined as HCO_3^- 176.8–213.2 $mg \cdot L^{-1}$ (70–79% eq), SO_4^{2-} 22.0–51.8 $mg \cdot L^{-1}$ (12–27% eq), and Cl^- 12.4–14.8 $mg \cdot L^{-1}$ (8–8.2% eq); and the content of ions were Ca^{2+} 26.1–32.1 $mg \cdot L^{-1}$ (27–36% eq), Mg^{2+} 14.1–17.6 $mg \cdot L^{-1}$ (24–28% eq), and Na^+ 39.7–56.9 $mg \cdot L^{-1}$ (34–48% eq).

At site S7, the Tsagan-gol River inflows into Lake Gusinoe. The TDS of the water samples varied from 63 to 86 $mg \cdot L^{-1}$; the content of anions was determined as HCO_3^- 48–52 $mg \cdot L^{-1}$, SO_4^{2-} 6.4–9.1 $mg \cdot L^{-1}$, and Cl^- 5.1–7.2 $mg \cdot L^{-1}$; and the content of ions was Ca^{2+} 11.2–14.5 $mg \cdot L^{-1}$, Mg^{2+} 1.5–1.8 $mg \cdot L^{-1}$, and Na^+ 12.3–15.4 $mg \cdot L^{-1}$. It is well known that the chemical composition of Tsagan-gol River water inherits the composition of the fractured-vein waters of the mountain frame and has a low mineralization. There is no anthropogenic activity in the watershed area of the Tsagan-gol River.

Following seasonal variation, the concentrations of Na^+ and SO_4^{2-} increased at sites S1–S6 during to the occurrence of open water, which is due to the input of river water under anthropogenic impact and the runoff of mine waters. Seasonal changes in the content of these ions differ more than 1.5–2 times In contrast, at site S7, where the Tsagan-gol River flows into the lake, the concentrations of these ions do not differ significantly [32].

Thus, the greatest impact of the anthropogenic impact on Lake Gusinoe occurred at sampling sites S1–S3. There was no anthropogenic impact on sampling site S7, except for the atmospheric transport of pollutants. Sampling sites S4–S6 were located far from the objects of the anthropogenic impact and were influenced by the processes of mixing and exchange with the water of the great lake.

Annually, water temperature ranged from 0 to 25.6 °C. The temperature of the water was higher during July (21–25.6 °C) and lower, at 0 °C, from November to April. The pH of the lake water ranged from 7.1 to 9.3 (average 8.6), indicating the alkaline conditions at all times and sampling sites.

Nutrients. Nutrient concentrations varied between different sampling sites and different seasons (Table 3). The highest TP (32 $\mu g \cdot L^{-1}$) and PO_4-P (19 $\mu g \cdot L^{-1}$) concentrations occurred during the winter at sampling site S3, which could reflect wastewater treatment plant (WWTP) releases and P diffusion from the sediments. The mean values of TP and and PO_4-P were 24–26 and 11–13 $\mu g \cdot L^{-1}$, respectively. Discharge from Gusioozersky WWTP could explain the warmer and denser waters occupying the near-bottom layer during the winter months. Sites S4–S7 exhibited lower TP concentrations (mean of 14–16 $\mu g \cdot L^{-1}$). Observations indicated that the TP content of Lake Gusinoe was changed significantly in space and with time. The highest concentrations of TP and PO_4-P at sampling sites S1–S3 were observed during the year. These sampling sites were under intense anthropogenic impact at the confluence of rivers Telya and Zagustai.

Table 3. Nutrient distribution for Lake Gusinoe waters during 2016–2018.

Station	PO_4-P	TP	NH_4-N	NO_3-N	Norg	TN
	$\mu g \cdot L^{-1}$	$\mu g \cdot L^{-1}$	$mg \cdot L^{-1}$	$mg \cdot L^{-1}$	$mg \cdot L^{-1}$	$mg \cdot L^{-1}$
			Winter			
S1	4–17	5–31	0–0.01	0.08–0.37	0.14–0.32	0.17–0.65
	11(5) *	24(19)	0.004 (0.003)	0.19 (0.22)	0.24 (0.19)	0.42 (0.38)
S2	2–15	12–32	0.002–0.008	0.12–0.35	0.17–0.42	0.27–0.54
	11(6)	21(17)	0.004 (0.005)	0.21 (0.18)	0.24 (0.18)	0.42 (0.38)
S3	2–19	12–32	0.002–0.004	0.17–0.47	0.16–0.38	0.25–0.56
	13(8)	24(19)	0.003 (0.005)	0.24 (0.28)	0.26(0.21)	0.48 (0.38)
S4	0–11	9–27	0–0.005	0.07–0.17	0.05–0.17	0.17–0.35
	7(5)	16(15)	0.002 (0.003)	0.11 (0.12)	0.14 (0.18)	0.25 (0.27)
S5	0–9	8–28	0–0.008	0.06–0.16	0.02–0.16	0.07–0.41
	6(5)	14(14)	0.003 (0.003)	0.09 (0.11)	0.12 (0.16)	0.26 (0.24)
S6	0–10	7–25	0–0.009	0.06–0.18	0.04–0.18	0.06–0.46
	7(5)	16(16)	0.004 (0.003)	0.08 (0.09)	0.12 (0.16)	0.29 (0.28)
S7	0–6	5–18	0–0.005	0.04–0.14	0.02–0.14	0.09–0.38
	4(5)	14(15)	0.002 (0.002)	0.06 (0.08)	0.09 (0.08)	0.19 (0.16)
			Spring			
S1	0–4	7–15	0.01–0.07	0.14–0.27	0.12–0.28	0.27–0.56
	2(3)	9(8)	0.02 (0.03)	0.24 (0.18)	0.18 (0.12)	0.37 (0.38)
S2	0–5	6–16	0.008–0.08	0.11–0.32	0.09–0.29	0.17–0.61
	2(3)	11(12)	0.04 (0.01)	0.28 (0.21)	0.21 (0.18)	0.41 (0.40)
S3	1–5	6–19	0.01–0.09	0.19–0.43	0.13–0.31	0.29–0.74
	3(4)	14(12)	0.04 (0.01)	0.31 (0.28)	0.28 (0.27)	0.44 (0.41)
S4	0–3	4–9	0.003–0.014	0.07–0.18	0.07–0.16	0.17–0.37
	2(5)	6(7)	0.008 (0.006)	0.11 (0.08)	0.09 (0.11)	0.28 (0.18)
S5	0–3	3–8	0.006–0.018	0.06–0.16	0.05–0.17	0.11–0.35
	1(2)	5(6)	0.009 (0.007)	0.12 (0.08)	0.11 (0.08)	0.31 (0.18)
S6	0–3	2–9	0.007–0.01	0.06–0.18	0.05–0.18	0.11–0.37
	1(2)	5(6)	0.009 (0.007)	0.11 (0.09)	0.11 (0.08)	0.29(0.18)
S7	0–2	1–6	0.002–0.008	0.02–0.08	0.02–0.07	0.05–0.17
	1(2)	4(6)	0.005 (0.004)	0.05 (0.06)	0.04 (0.02)	0.12 (0.08)
			Summer			
S1	2–7	5–12	0.008–0.015	0.11–0.21	0.12–0.27	0.12–0.49
	4(4)	9(8)	0.011 (0.01)	0.15 (0.12)	0.19 (0.18)	0.26 (0.32)
S2	2–9	4–14	0.01–0.018	0.09–0.27	0.09–0.28	0.11–0.56
	5(4)	11(8)	0.015 (0.012)	0.18 (0.15)	0.21 (0.2)	0.24 (0.38)
S3	1–11	5–18	0.01–0.021	0.12–0.31	0.12–0.31	0.14–0.65
	6(5)	12(9)	0.018 (0.016)	0.21 (0.18)	0.25 (0.21)	0.28(0.43)
S4	1–4	3–9	0.004–0.011	0.07–0.14	0.06–0.17	0.12–0.31
	3(2)	7(6)	0.006 (0.005)	0.11 (0.12)	0.12 (0.11)	0.15 (0.21)

Table 3. *Cont.*

Station	PO_4-P	TP	NH_4-N	NO_3-N	Norg	TN
	$\mu g \cdot L^{-1}$	$\mu g \cdot L^{-1}$	$mg \cdot L^{-1}$	$mg \cdot L^{-1}$	$mg \cdot L^{-1}$	$mg \cdot L^{-1}$
S5	0–5 3(2)	2–8 6(6)	0.003–0.009 0.007 (0.006)	0.06–0.15 0.09 (0.08)	0.07–0.17 0.13 (0.12)	0.11–0.32 0.12 (0.23)
S6	2–6 5(2)	2–8 6(5)	0.002–0.008 0.005 (0.005)	0.07–0.13 0.11 (0.08)	0.06–0.16 0.14 (0.13)	0.13–0.28 0.16 (0.25)
S7	0–4 2(2)	1–8 5(6)	0–0.008 0.003 (0.001)	0.04–0.07 0.05 (0.04)	0.03–0.07 0.05 (0.04)	0.06–0.14 0.12 (0.11)

Note: * In the numerator—ranges, in the denominator—mean value, bracket values are S.D.

The distribution of N in Lake Gusinoe exhibited a distinctive pattern (Table 3). The concentration of NO_3-N resembled that of Norg (~0.2 mg L^{-1}) and was the highest value (0.47 $mg \cdot L^{-1}$) in the winter. The NH_4-N concentration was low (0.006–0.008 mg L^{-1}). The highest value of NH_4-N (0.07–0.09 $mg \cdot L^{-1}$) was determined in the spring. The concentration of NO_2-N was 0–0.002 $mg \cdot L^{-1}$ and did not vary significantly in terms of time and space. The highest value of TN was 65 $mg \cdot L^{-1}$ at site S1 in the winter.

In order to highlight the difference between sampling sites, statistics multiple regression was applied. Figure 2 displays a significantly different distribution between the winter and water-open period of the obtained values, especially for P-PO_4, N-NH_4, and N-NO_3. Higher concentrations were registered for P-PO_4 and N-NO_3 during the winter. The high concentration values of TP and TN could be observed at sampling sites S1-S3 during all the seasons. In the open-water period there, were no important seasonal or spatial variations in the P-PO_4 and N-NO_3 concentrations.

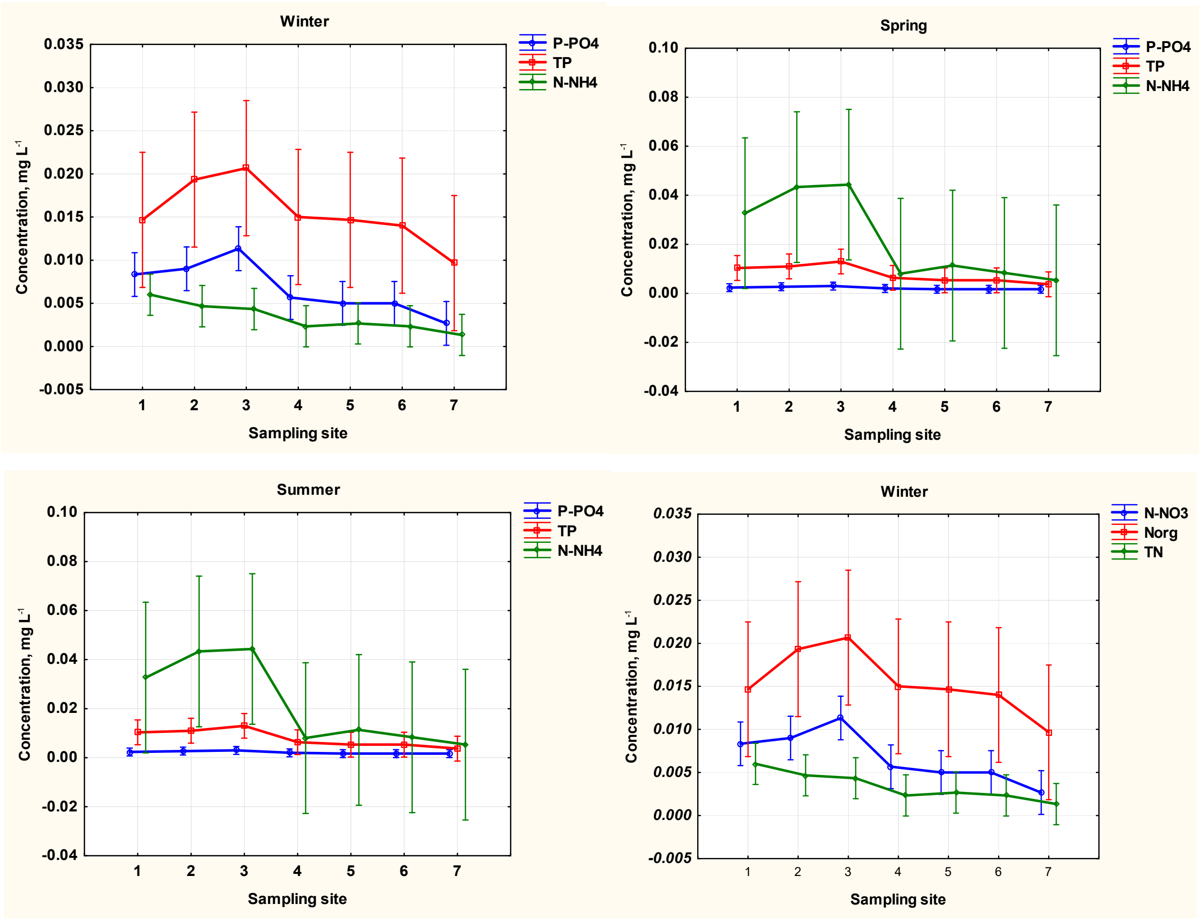

Figure 2. *Cont.*

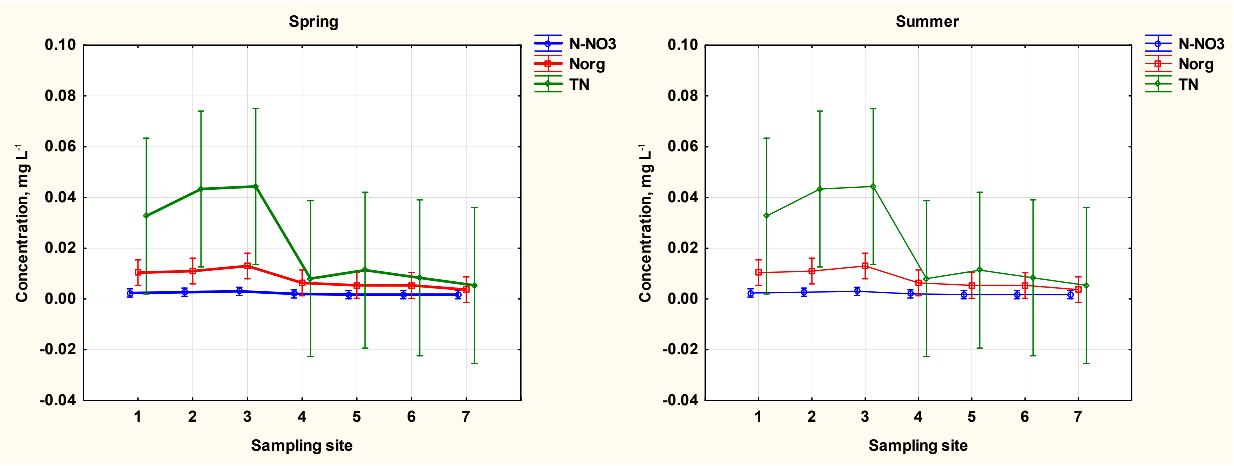

Figure 2. The distribution pattern of nutrients in Lake Gusinoe during the year.

Organic matter. The organic matter (OM) concentrations varied considerably between different samples (Table 4). The OM composition during ice-free periods depended largely on the annual precipitation and hydrometeorological conditions, which control the intensity of the water exchange. Given the high precipitation during the spring of 2017, there were elevated levels of dissolved oxygen, DO (11.8 mg·L^{-1}), chemical oxygen demand, COD (21.8 mg·L^{-1}), and total organic carbon, TOC (16.2 mg·L^{-1}), content. The concentrations of the chemical oxygen demand (COD) and biological oxygen demand (BOD_5) were much higher in the summer, at 36,5 and 5.3 mg·L^{-1}, respectively, compared to those measured in the winter. At the same time, for example, the concentration of dissolved oxygen (DO) exhibited a decrease in the highest concentrations from 10.8–11.8 to 9.3–9.8 mg·L^{-1} at sites S1–S3. The results of the statistics multiple regression are displayed in Figure 3. The distribution pattern indicates that organic matter (OM) concentrations were at the highest values at sites S1–S3.

Table 4. Dissolved oxygen, total organic carbon, and chemical and biological oxygen, including the elemental composition of the water samples from Lake Gusinoe in 2016–2018, measured in mg·L^{-1}.

Station	DO	TOC	COD_{Cr}	BOD_5	C/N	C/P
			Winter			
S1	7.1–10.2 8.3(2.2) *	6.5–9.8 7.2(3.2)	8.3–13.2 10.1 (1.3)	1.8–3.6 2.3 (1.1)	17	300
S2	7.2–11.8 8.1(2.4)	5.8–9.2 7.3(2.9)	7.6–15.4 11.4 (1.6)	2.1–3.5 2.6 (1.3)	17	347
S3	7.3–11.7 8.2(2.4)	4.5–9.6 8.4(3.5)	8.3–12.5 12.5 (1.7)	1.6–4.1 2.9 (1.3)	18	350
S4	7.8–11.2 8.8(2.4)	3.8–7.8 5.6(2.9)	6.2–9.4 7.8 (2.1)	1.2–2.6 1.8 (1.2)	22	350
S5	7.8–12.8 8.5(2.2)	3.7–6.3 5.2(2.7)	5.7–10.2 7.3 (1.8)	1.7–2.7 2.1 (1.2)	20	371
S6	7.6–11.4 8.4(2.6)	4.3–6.7 5.4(2.7)	6.4–9.8 8.1 (1.7)	1.5–2.3 1.9 (1.1)	18	337
S7	7.8–12.2 8.5(2.7)	4.5–7.1 5.1(3.1)	5.8–12.4 6.7 (1.5)	1.1–1.8 1.6 (1.2)	27	364
			Spring			
S1	9.8–12.3 10.2(2.5)	9.6–16.8 10.2(2.8)	10.2–19.4 16.4 (3.2)	2.7–4.2 3.5 (0.82)	28	1130
S2	9.6–12.6 10.2(2.8)	9.2–18.2 11.3(2.9)	9.8–21.6 17.8 (3.2)	2.5–4.6 3.6 (0.84)	28	1027

Table 4. *Cont.*

Station	DO	TOC	COD$_{Cr}$	BOD$_5$	C/N	C/P
S3	9.7–12.6 10.4(2.4)	8.6–18.3 12.4(3.1)	10.3–22.7 18.6 (2.9)	2.9–5.2 3.9 (0.86)	28	885
S4	8.9–11.8 9.4(2.1)	6.7–14.8 8.2(2.7)	9.8–18.4 11.2 (3.1)	2.1–3.6 2.7 (0.67)	29	1366
S5	8.7–10.9 9.7(2.3)	7.2–15.3 8.6(2.6)	9.4–17.6 12.1 (2.9)	2.1–3.5 2.9 (0.64)	27	1720
S6	8.3–11.1 9.6(2.4)	6.3–14.7 8.7(2.7)	9.4–18.4 12.3 (3.1)	1.9–3.2 2.6 (0.71)	30	1740
S7	8.5–11.2 10.2(2.3)	5.6–15.1 7.8(2.5)	6.2–16.2 9.8 (2.7)	1.9–2.9 2.4 (0.52)	65	1950
Summer						
S1	7.4–9.3 8.6(2.9)	8.2–14.3 9.6(3.2)	10.6–26.4 20.7 (1.8)	1.9–4.8 3.8 (0.95)	26	1066
S2	7.2–9.8 8.1(2.5)	7.8–15.2 10.5(2.9)	12.3–34.2 24.2 (1.9)	2.4–5.2 4.1 (0.89)	24	954
S3	7.4–9.5 8.3(2.7)	8.2–16.4 13.6(3.5)	11.8–36.5 25.1 (1.7)	2.4–5.3 4.2 (0.91)	27	1133
S4	8.2–10.6 8.8(2.2)	6.8–12.6 9.1(2.9)	9.8–20.4 15.8 (1.5)	1.9–4.2 3.1 (0.73)	38	1300
S5	8.4–11.6 9.1(2.3)	5.7–12.3 8.6(2.7)	10.3–22.1 14.9 (1.6)	2.1–3.6 2.9 (0.74)	34	1437
S6	8.2–10.5 8.9(2.1)	6.3–12.7 9.2(2.7)	11.1–23.4 16.4 (1.4)	1.9–3.9 2.9 (0.84)	35	1533
S7	8.6–9.4 9.1(2.1)	5.6–14.2 8.4(3.1)	9.5–18.6 13.7 (1.3)	1.6–3.4 2.7 (0.91)	70	1680

Note: In the numerator—range; in the denominator—mean, * bracket values are S.D.

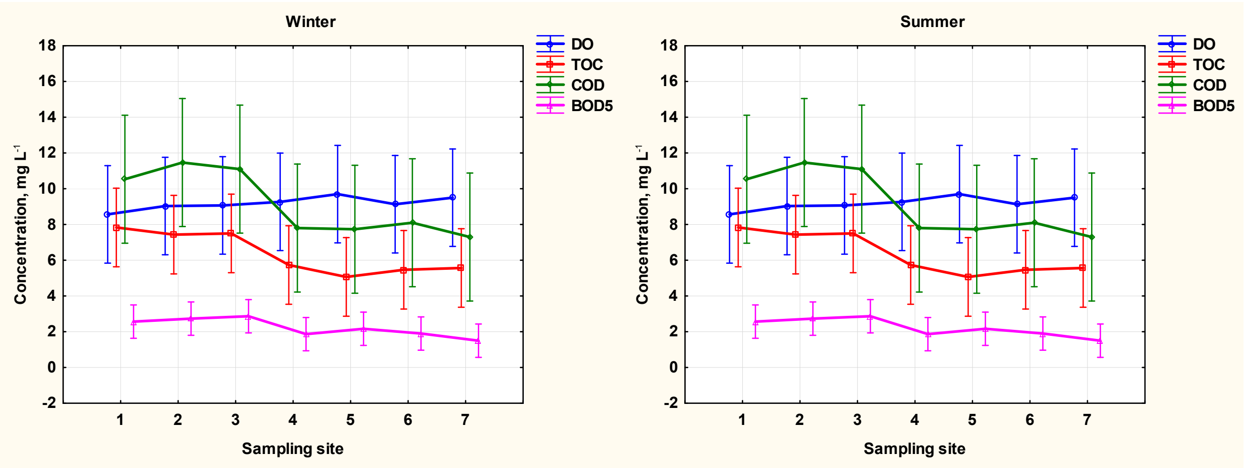

Figure 3. The distribution pattern of the dissolved oxygen and organic matter concentrations at Lake Gusinoe during the year.

At sampling sites S1–S3, the content of the organic matter and nutrients were increased and higher by almost two times than that in sites S4–S7. In contrast, the dissolved oxygen (DO) was decreased by 1.25 times as a result of production and destruction biological processes (Figure 4). At same time the pH values showed less variation, ranging from 7.1 to 9.12.

There were significant differences in the distribution of mass ratios C/N and C/P depending on the sampling site (Table 4). The highest value of ratios C/N (70) and C/P (1950) were observed in the spring and summer at site S7, higher by 1.1–1.4 times than that of the values in other sampling sites.

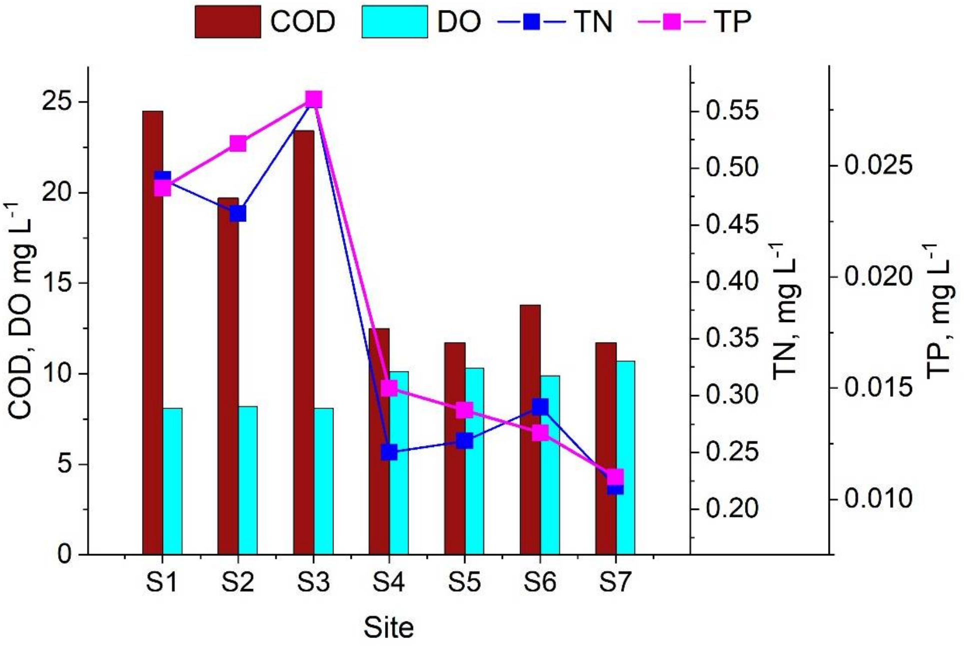

Figure 4. The varying concentrations of dissolved oxygen, chemical oxygen demand, total nitrogen, and total phosphorus at the sampling sites in the summer of 2016.

The monitoring data were compared with the Russian standard from the hygienic norms, specifically "Maximal Permissible Concentration of Chemical Substances in water of the Water Sources of Drinking and Communal use" [31]. Figure 5 illustrates the weights of the six parameters analyzed at the seasonal value of WPI, with these parameters established according to the result of the C_i/MPC_i (see Equation (1)). According to the graphic representations, the weight of the parameters varies from one season to another. BOD_5 and DO contribute, to the largest extent, to the final results of WPI, as recorded in all seasons. This is because these variables significantly exceeded the maximum permissible concentration in different seasons. In the summer, the contribution of $N\text{-}NH_4$ had an important contribution to WPI. This is explained by the fact that in open water, the content of $N\text{-}NH_4$ increased. However, the WPI index did not have a high sensitivity for different sampling sites in Lake Gusinoe. The authors of the works [33,34] showed that the WPI can be used particularly to determine the level of pollution, with the results showing only the exceedances of the maximum allowed concentrations. The value of WPI varied between 0.22 0.29 at all sampling sites during the year. Currently, according to the Russian water quality classification based on WPI [31], the water of Lake Gusinoe is pure.

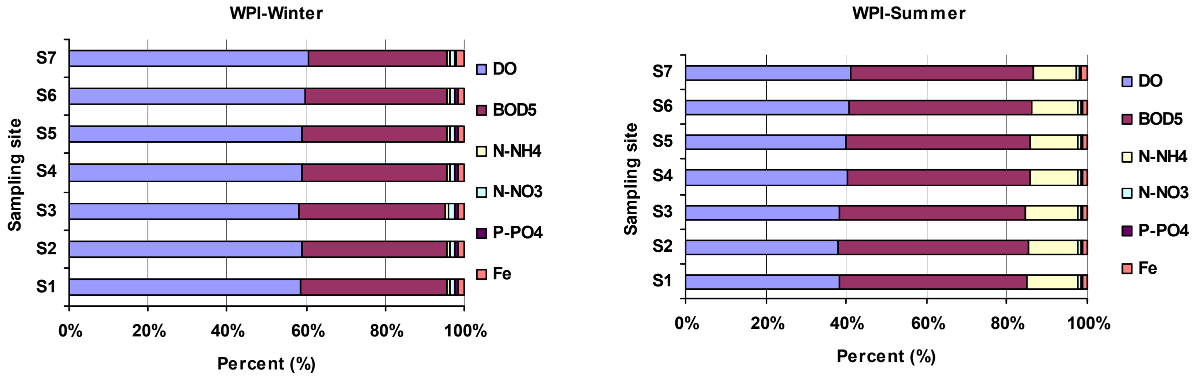

(**a**) (**b**)

Figure 5. The weight of each parameter to the WPI values recorded in winter (**a**) and summer (**b**).

In this study, the variables of nutrients and organic matter in the lake were identified. The results suggest that anthropogenic activities had significant effects on the water. The power electricity industry and WWTP of Gusinoozersk presented serious negative feedbacks for water pollution.

Trace element. The input of chemical elements into lake water is controlled mainly by the supply ground, surface waters, and antropogenic impact, and their further concentration is determined by the processes of vaporization, by the physico-chemical properties of the elements themselves, and by the geochemical conditions of the environment. The saturation of supply water with trace elements depends on their extraction from rocks, which is controlled by the processes of the water–rock interaction [35–39].

Trace element concentrations in the lake water spanned with 6–7 orders of magnitude. The maximum concentrations within n 100 $\mu g \cdot L^{-1}$ were observed for Sr. The concentrations within n 10 $\mu g \cdot L^{-1}$ were typical for Li and Mo, as well as within n $\mu g \cdot L^{-1}$- for Al, Mn, Cu, Zn, Rb, and U; within n 0.1 $\mu g \cdot L^{-1}$ for V, Ni, As, W, Cd, and Pb; within n 0.01 $\mu g \cdot L^{-1}$ for Co, Ga, Ge, Y, La, Ce, Pr, and Nd; and within n 0.001 $\mu g \cdot L^{-1}$ for Ga, Th, Sm, Eu, Gd, Tb, Dy, Er, and Yb (Table 5).

Table 5. The mean value of the trace element concentrations of the Gusinoe Lake in July–August during 2016–2018; $n = 9$—number of samples ($\mu g \cdot L^{-1}$).

Element	S1	S2	S3	S4	S5	S6	S7	Detection Limit
Li	20.21	19.41	19.59	19.38	20.07	19.45	1.38	0.057
Al	4.31	3.48	3.94	2.30	2.72	4.13	5.86	2.62
V	0.979	0.834	0.799	0.751	0.801	0.742	0.054	0.0035
Cr	0.047	0.045	0.035	0.035	0.041	0.036	0.066	0.017
Mn	1.09	1.65	2.39	1.11	0.54	0.28	0.56	0.024
Fe	2.10	3.82	5.20	1.59	1.11	1.06	103.59	0.56
Co	0.02	0.02	0.02	0.02	0.02	0.02	0.03	0.0014
Ni	0.26	0.30	0.29	0.25	0.31	0.28	0.20	0.024
Cu	1.01	1.61	1.47	0.89	1.16	0.77	0.40	0.052
Zn	0.99	1.06	1.16	4.63	1.46	0.96	1.26	0.12
Ga	0.014	0.008	0.008	0.004	0.006	0.005	0.001	0.0135
Ge	0.029	0.033	0.018	0.022	0.020	0.021	0.007	0.0024
As	0.992	0.987	0.994	0.985	1.013	0.935	0.160	0.011
Rb	1.31	1.25	1.24	1.21	1.28	1.25	0.59	0.0087
Sr	952.08	929.46	925.36	920.69	961.00	938.19	99.07	0.14
Y	0.0266	0.0188	0.0183	0.0153	0.0162	0.0197	0.0312	0.0006
Nb	0.0448	0.0025	0.0020	0.0017	0.0018	0.0039	0.0053	0.0032
Mo	16.15	13.99	13.01	13.04	13.15	13.12	0.65	0.057
Cd	0.101	0.098	0.088	0.082	0.096	0.083	0.025	0.0016
Ba	20.80	20.37	20.23	20.28	21.40	21.13	9.01	0.040
La	0.0184	0.0392	0.0133	0.0101	0.0095	0.0119	0.0355	0.011
Ce	0.0183	0.0232	0.0239	0.0098	0.0060	0.0421	0.0291	0.0022
Pr	0.0401	0.0020	0.0019	0.0014	0.0015	0.0031	0.0074	0.0003
Nd	0.0178	0.0087	0.0076	0.0058	0.0066	0.0080	0.0343	0.0020
Sm	0.0039	0.0049	0.0046	0.0026	0.0043	0.0056	0.0095	0.0003
Eu	0.0116	0.0106	0.0102	0.0096	0.0102	0.0101	0.0057	0.0004
Gd	0.0052	0.0038	0.0042	0.0039	0.0052	0.0034	0.0083	0.0003
Tb	0.0005	0.0006	0.0007	0.0007	0.0006	0.0007	0.0016	0.0009
Dy	0.0048	0.0044	0.0030	0.0031	0.0032	0.0046	0.0073	0.0002
Ho	0.0011	0.0008	0.0006	0.0006	0.0007	0.0010	0.0016	0.0003
Er	0.0045	0.0021	0.0022	0.0026	0.0022	0.0026	0.0051	0.0006
Tm	0.0012	0.0006	0.0008	0.0006	0.0006	0.0006	0.0009	0.0001
Yb	0.0057	0.0028	0.0024	0.0033	0.0025	0.0034	0.0057	0.0005
Lu	0.0011	0.0006	0.0008	0.0006	0.0007	0.0007	0.0013	0.0005
Ta	0.0350	0.0004	0.0003	0.0003	0.0004	0.0004	0.0003	0.0002
W	0.560	0.418	0.415	0.422	0.394	0.399	0.012	0.011

Table 5. *Cont.*

Element	S1	S2	S3	S4	S5	S6	S7	Detection Limit
Pb	0.149	0.183	0.083	0.077	0.177	0.401	0.110	0.014
Th	0.0082	0.0027	0.0034	0.0013	0.0030	0.0023	0.0088	0.0018
U	1.819	1.696	1.905	1.690	1.274	1.452	0.102	0.011
ΣLREE	0.016	0.011	0.010	0.009	0.010	0.011	0.010	
ΣHREE	0.011	0.007	0.007	0.007	0.007	0.008	0.014	
ΣREE	0.028	0.018	0.018	0.016	0.017	0.018	0.024	
Ce/Ce*	0.089	0.429	0.997	0.543	0.342	1.504	0.390	
Eu/Eu*	11.088	10.704	10.208	12.779	9.411	10.010	2.818	
$(La/Yb)_N$	0.312	1.358	0.531	0.294	0.362	0.340	0.606	

In accordance with the behavior of elements in the waters feeding the lake and in the process of evaporation of lake water, three groups of elements could be distinguished. As shown in [32], the smallest TDS was determined at site S7. A clear distinction existed between trace elements whose abundance followed the abundance of major elements or TDS, and whose concentrations were decoupled from the variations of major ions. In Lake Gusinoe, three categories were revealed. The first set of elements, including Li, Ga, Ge, As, Rb, Sr, Mo, Cd, Ba, W, and U, were directly correlated with variations of major elements. The first set of elements showed decreasing concentrations with increasing TDS (site S1–S6). The second set of elements, including Fe, Y, Nb, Th, and REE, were correlated oppositely with variations of TDS, in contrast to the elements of the first set. The behavior of the third set of elements, including Mn, Zn, Ni, Cu, and Pb, decoupled from the major elements and their variations at the sampling sites were not correlated with TDS.

In order to assess the processes of vaporization and the anthropogenic impact, the concentration ratio of the trace elements at sites S1, S5, S6, and S7 were calculated. Sampling sites S1, S5, and S6 represented the anthropogenic impact and the central part of the lake with missing waters. Figure 6 displays the distribution of the concentration ratios.

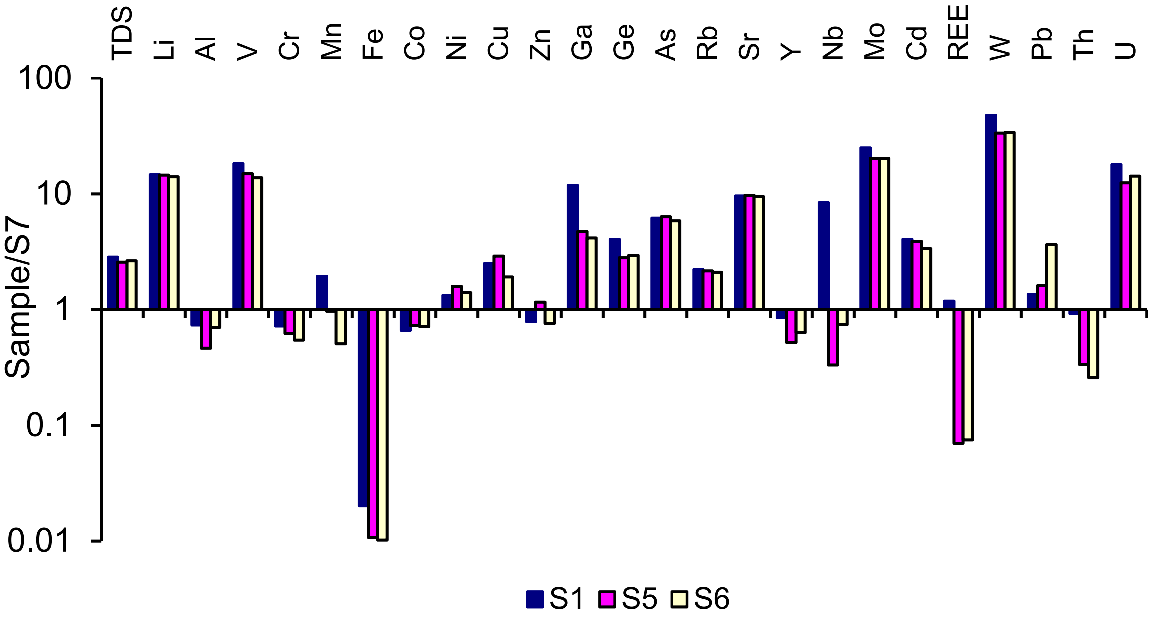

Figure 6. The distribution of the concentration ratios at different sampling sites.

The highest obtained values were for W (33.6–47.7), Mo (20–24.9), V (13–18), U (12.4–17.8), Li (14–14.6), Sr (9.4–9.7), and Ga (94.1–11.8). The water of the lake was extremely enriched by these elements. The elements Al, Cr, Mn, Fe, Co, Zn, Y, Th, and REE had values of less than 1.0. These elements minimally accumulated in the lake water. The enrichment elements

Ni, Cu, Ge, As, Rb, Cd, and Pb had values of between 1.4 and 6.3, and thus they moderately accumulated in the water of Lake Gusinoe.

Generally, elements known to be present as oxyanions (As, Mo, W, U, and others) in oxidized water exhibit some coherence with major solute variations. The best examples of decoupling between major solutes and trace elements derive from REEs. As shown in [37], the lowest concentrations of REEs in river waters are found in the rivers with the highest pH. In Lake Gusinoe at sites S1–S6, as they are greatly influenced by carbonate dissolution, high pH and alkalinity values were determined and found to be present at very low REE concentrations, in contrast to site S7. Elements such as Th and Y, and to a lesser extent Fe, Al, Mn, and Zn, are correlated with REE concentrations in lake water. The close association of these elements with DOC has been shown by other authors [38,39].

Total concentrations of Al, Fe, and Mn showed increases across the sites, with higher values in the northern sites (S1–S3) compared to the other sites (S4–S7). The differences between the particulate and dissolved concentrations were highest for Al, Fe, and Mn, with particulate concentrations that were, on average, 57, 28, and 24 times greater, respectively, than the dissolved concentrations in the 2016 monitoring campaign, and 36, 12, and 8 times greater, respectively, in the 2017 campaign. As, Cd, Cr, Cu, and Mo had dissolved concentrations of the same order of magnitude as their total concentrations. V and Zn showed varying behaviors, exhibiting both higher dissolved and particulate concentrations depending on the sampling site.

As shown in [40,41], the precipitation of gibbsite and ferrihydrite was predicted to be the dominant control of Al and Fe, with these particulate fractions generally limiting their solubility by 90–100%. In others works [42–44], 40–50% was predicted to occur as soluble organic complexes (bound to DOC). In other locations, only minor fractions of Fe (up to 10%) were predicted to exist as complexes with organic matter. Metal–organic complexation also had a large impact on the speciation of Pb and Zn, and these elements were predicted to form soluble complexes with DOC, on average, governing their speciation by 50% and 30%, respectively. Sorption processes to ferrihydrite and gibbsite mainly controlled the solubility of V, Pb, and Zn. V, Cr, and Pb were predicted to sorb only to ferrihydrite, on average, by 60%, while Zn was predicted to sorb to both ferrihydrite and gibbsite (on average, by 65%), but with predominant sorption to gibbsite over ferrihydrite (under pH conditions above 8).

The content of REE and their fractionation degree by indicator $(La/Yb)_N$ is presented in Table 5. The total content varied for $\Sigma REE = 0.016–0.024\ \mu g \cdot L^{-1}$. In the REE patterns for most sampling sites, HREE strongly dominated over LREE: $(La/Yb)_N = 0.29–0.60$. The exception was water from site S2, where $(La/Yb)_N = 1.35$. The content of Σ HREE was higher at site S7 by 1.2–2.0 times than at other sites.

There was a difference in the value and sign of the Ce and Eu anomaly. The distribution of REE when normalized to NASC [45] is shown in Figure 7. Cerium anomalies were not observed at sites S1-S5 ($Ce/Ce^* = 0.089–0.342$). The negative anomaly $Ce/Ce^* = 1.504$ was recorded at site S6, which was due to the mine water of the coal-bearing Cholboldze deposit. The REE normalized profile was characterized by deeper positive anomalies ($Eu/Eu^* = 2.8–12.7$). The lowest value ($Eu/Eu^* = 2.818$) derived from the water from site S7, where the anthropogenic impact was minimal. The value of the Eu anomaly was positive correlated with TDS. From these results, it follows that the Eu anomaly is an indicator of anthropogenic influence and of the process of vaporization in Lake Gusinoe.

The Malo-Khamardaban volcanogenic association is one of the largest and typomorphic structures of the Jurassic–Cretaceous rift magmatism of the western Transbaikalia. It is mainly made up of bimodal volcanogenic trachybasalt–trachyte series with subordinate amounts of trachyandesites, trachyrhyodacites, and trachyrhyolites. As shown by several authors [46–48], the mineralogical–petrographic, mineralogical–geochemical, and geochemical features of trachyandesites as well as of some syenite porphyries (subvolcanic analogues of trachytes) indicate their hybrid nature. The trachyandesites were formed by mixing trachybasaltic magma with trachytic magmas (endohybridisation), and trachybasaltic magma with contaminated trachytic magma. Trachybasalts and trachytes contain weak positive Eu anomalies (Eu/Eu* = 1.24–0.84) for the normalized primitive mantle.

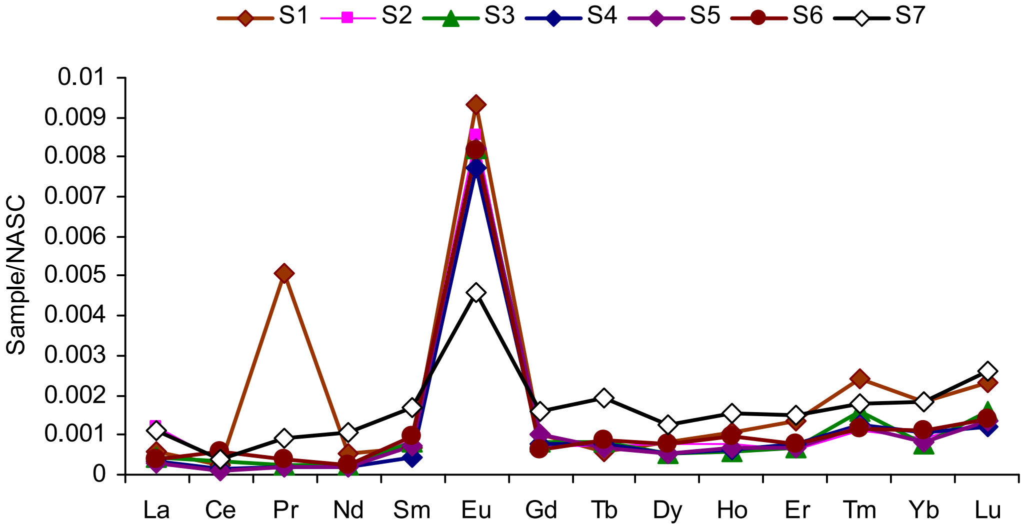

Figure 7. Normalized distribution of rare earth elements in the lake water.

4. Conclusions

Lake Gusinoe is the second largest freshwater lake in Transbaikalia. Lakes serve as a source of drinking water and irrigation, and as a water source for the electricity, aquatic production, and tourism industry. The electricity industry and sewages discharges both affect water quality. The combined influence of these two main sources depends on the intensity of the bay–lake exchange, which in turn varies with annual precipitation and hydrometeorological conditions. In the winter, the hydrochemical regime depends primarily on the Telya and Zagustai River inflow because the water exchange between the bay and the central lake is restricted during its ice-covered period. In this period, the content of nutrients was highest for TP (32 $\mu g \cdot L^{-1}$) and TN (0.65 mg L^{-1}), while DO saturation varied from 72% to 98%. In the spring, summer, and autumn, when bay water masses experience wind-induced and thermal mixing, open lake water exerts the strongest influence on chemical composition, evident by the lower mean concentrations of TP (9–11 $\mu g \cdot L^{-1}$), TN (0.24–0.26 $mg \cdot L^{-1}$), and DO (8.1–8.3 $mg \cdot L^{-1}$), as well as by the highest content of COD (36.5 $mg \cdot L^{-1}$) and BOD_5 ($mg \cdot L^{-1}$).

Seasonal monitoring indicated that sewage from power stations and Gusinoozersk, which bothndischarge sewage into the peripheral areas of the lake, exerted only minor effects on the bay water quality during the spring and autumn period of mixing with open waters of the greater lake. In water sample sites S1–S3, which were under the anthropogenic impact, the content of the organic matter and nutrients were increased by almost 2 times compared to other sampling sites which had less influence from pollution sources.

The water of Lake Gusinoe is extremely enriched by W, Mo, V, U, Li, Sr, and Ga; moderately by Ni, Cu, Ge, As, Rb, Cd, and Pb; and minimally by Al, Cr, Mn, Fe, Co, Zn, Y, Th, and REE. In most areas of the water, HREE strongly dominated over LREE. The cerium anomaly was not observed in most of the lake, except for the area where mine waters of the coal-bearing Cholboldze deposit inflow. The normalized distribution of REE was characterized by a deeper positive Eu anomaly, which was due to the geochemical features of trachybasalts and trachytes of the Malo-Khamardaban volcanogenic association.

Author Contributions: Z.I.K. wrote the text and conducted both the data curation and formal analysis; A.M.P. assisted in the research and provided funding; O.K.S. wrote, reviewed, and edited the manuscript; E.G.P. wrote the original draft; S.S.S. assisted in the research and chemical analysis; D.I.Z., S.G.D. and V.V.D. conducted the sample preparation. All authors have read and agreed to the published version of the manuscript.

Funding: This study was performed within the state tasks of GIN SB RAS. The investigations have been conducted within the fundamental research framework of the GIN SB RAS (registered number AAAA-A21-121011890033-1).

Institutional Review Board Statement: The studies were carried out in accordance with the state assignment of the Siberian Branch of the Russian Academy of Sciences.

Informed Consent Statement: The consent of the expert commission of the Geological Institute on the publication and access of data in the open press is available.

Data Availability Statement: Permission for publication in the open press is available.

Conflicts of Interest: The authors declare no conflict of interest.

References

1. Borisenko, I.M.; Pronin, N.M.; Shibonov, B.B. *Ecology of Lake Gusinoe Izd*; BNTs SO RAN: Ulan-Ude, Russia, 1994; 186p. (In Russian)
2. Bulnaev, K.B. The formation of "Transbaikal type" depressions. *Tikhookeanskaya Geol.* **2006**, *25*, 18–30.
3. Lunina, O.V.; Gladkov, A.S. Fault-block structure and state of stress in the Earth's crust of the Gusinoozersky basin and the adjacent territory, Western Transbaikal region. *Geotectonics* **2009**, *43*, 67–84. [CrossRef]
4. Doroshkevich, A.G.; Kobylkina, O.V.; Ripp, G.S. Role of sulfates in the formation of carbonatites in the western Transbaikal region. *Dokl. Earth Sci.* **2003**, *388*, 131–134.
5. Ripp, G.S.; Khodanovich, P.Y.; Smirnova, O.K. A new carbontite province in West Transbaikalia. *Russ. Geol. Geophys.* **1999**, *40*, 73–81.
6. Borkhonova, E.V. Flooding of Built-Up Areas in the Intermontane Depressions of Western Transbaikalia. Ph.D. Thesis, Publishing House of Buryat State University, Ulan-Ude, Russia, 2006; 35p.
7. Sayers, M.; Bosse, K.; Fahnenstiel, G.; Shuchman, R. Carbon Fixation Trends in Eleven of the World's Largest Lakes: 2003–2018. *Water* **2020**, *12*, 3500. [CrossRef]
8. Mohamed, N.; Wellen, C.; Parsons, C.T.; Taylor, W.D.; Arhonditsis, G.; Chomicki, K.M.; Boyd, D.; Weidman, P.; Mundle, S.O.C.; van Cappellen, P.; et al. Understanding and managing the re-eutrophication of Lake Erie: Knowledge gaps and research priorities. *Freshw. Sci.* **2019**, *38*, 675–691. [CrossRef]
9. Bootsma, H.A. Oceans, Lakes, and Inland Seas: A Virtual Issue on the Large Lakes of the World. *Limnol. Oceanogr. Bull.* **2018**, *27*, 87–88. [CrossRef]
10. Lau, S.S.; Lane, S.N. Biological and chemical factors influencing shallow lake eutrophication: A lond-term study. *Sci. Total Environ.* **2002**, *228*, 167–181. [CrossRef]
11. Filatov, N.N. (Ed.) *The Largest Lakes-Reservoirs of the Northwest European Part of Russia: Current State and Changes of Ecosystems under Climate Variability and Anthropogenic Impact*; Publishing House of Karelian Research Center of the Russian Academy of Sciences: Petrozavodsk, Russia, 2015; 200p. (In Russian)
12. Efremova, T.A.; Sabylina, A.V.; Lozovik, P.A.; Zobkova, M.V.; Pasche, N. Seasonal and spatial variation in hydrochemical parameters of Lake Onego (Russia): Insights from 2016 field monitoring. *Inland Waters* **2019**, *9*, 227–238. [CrossRef]
13. Lozovik, P.A.; Zobkova, M.V.; Ryzhakov, A.V.; Zobkov, M.B.; Efremova, T.; Sabylina, A.V.; Efremova, T.V. Allochthonous and autochthonous organic matter in natural waters: Kinetic and thermodynamic patterns of transformation and quantitative and qualitative compositions. *Dokl. Earth Sci.* **2017**, *477*, 1510–1514. [CrossRef]
14. Belkina, N.A. Phosphorus in the sediments of the Lake Onega. Izvestia: Herzen University. *J. Humanit. Sci.* **2015**, *173*, 97–109. (In Russian)
15. Lozovik, P.A.; Zobkov, M.B.; Borodulina, G.S.; Tokarev, I.V. Assessing external water exchange of lake bays by water chemistry characteristics. *Water Resour.* **2019**, *46*, 91–101. [CrossRef]
16. Bouffard, D.; Zdorovennov, R.E.; Zdorovennova, G.E.; Pasche, N.; Wüest, A.; Terzhevik, A.Y. Ice-covered Lake Onega: Effects of radiation on convection and internal waves. *Hydrobiologia* **2016**, *780*, 21–26. [CrossRef]
17. Mahdiyan, O.; Filazzola, A.; Molot, L.A.; Gray, D.; Sharma, S. Drivers of water quality changes within the Laurentian Great Lakes region over the past 40 years. *Limnol. Oceanogr.* **2020**, *66*, 237–254. [CrossRef]
18. Guiry, E.J.; Buckley, M.; Orchard, T.J.; Hawkins, A.L.; Needs-Howarth, S.; Holm, E.; Szpak, P. Deforestation caused abrupt shift in Great Lakes nitrogen cycle. *Limnol. Oceanogr.* **2020**, *65*, 1921–1935. [CrossRef]
19. Scavia, D.; Anderson, E.J.; Dove, A.; Hill, B.; Long, C.M.; Wang, Y. Lake Huron's Phosphorus Contributions to the St. Clair–Detroit River Great Lakes Connecting Channel. *Environ. Sci. Technol.* **2020**, *54*, 5550–5559. [CrossRef]
20. Fraker, M.E.; Shrestha, A.; Marshall, L.; Mason, L.; Miller, R. Seasonal variation in light penetration and subsurface chlorophyll-α in southern Lake Michigan observed by a glider. *J. Great Lakes Res.* **2021**, *47*, 1228–1234. [CrossRef]
21. Chorus, I.; Köhler, A.; Beulker, C.; Fastner, J.; van de Weyer, K.; Hegewald, T.; Hupfer, M. Decades needed for ecosystem components to respond to a sharp and drastic phosphorus load reduction. *Hydrobiologia* **2020**, *847*, 4621–4651. [CrossRef]
22. Pothoven, S.A.; Vanderploeg, H.A. Seasonal patterns for Secchi depth, chlorophyll a, total phosphorus, and nutrient limitation differ between nearshore and offshore in Lake Michigan. *J. Great Lakes Res.* **2020**, *46*, 519–527. [CrossRef]

23. Larson, J.H.; James, W.F.; Fitzpatrick, F.A.; Frost, P.C.; Evans, M.A.; Reneau, P.C.; Xenopoulos, M.A. Phosphorus, nitrogen and dissolved organic carbon fluxes from sediments in freshwater rivermouths entering Green Bay (Lake Michigan; USA). *Biogeochemistry* **2020**, *147*, 179–197. [CrossRef]
24. Burlakova, L.E.; Barbiero, R.P.; Karatayev, A.Y.; Daniel, S.E.; Hinchey, E.K.; Warren, G.J. The benthic community of the Laurentian Great Lakes: Analysis of spatial gradients and temporal trends from 1998 to 2014. *J. Great Lakes Res.* **2018**, *44*, 600–617. [CrossRef] [PubMed]
25. Sgro, G.V.; Reavie, E.D. Fossil diatoms, geochemistry, and the Anthropocene paleolimnology of Lake Huron. *J. Great Lakes Res.* **2018**, *44*, 765–778. [CrossRef]
26. Li, J.; Ianaiev, V.; Huff, A.; Zalusky, J.; Ozersky, T.; Katsev, S. Benthic invaders control the phosphorus cycle in the world's largest freshwater ecosystem. *Proc. Natl. Acad. Sci. USA* **2021**, *118*, e2008223118. [CrossRef]
27. Ciesielski, T.M.; Pastukhov, M.V.; Leeves, S.A.; Farkas, J.; Lierhagen, S.; Poletaeva, V.; Jenssen, B.M. Differential bioaccumulation of potentially toxic elements in benthic and pelagic food chains in Lake Baikal. *Environ. Sci Pollut. Res.* **2016**, *23*, 15593–15604. [CrossRef] [PubMed]
28. Stroganov, M.C.; Buzinova, N.C. *A Practical Guide to Hydrochemistry*; Publishing House of Moscow State University: Moscow, Russia, 1980; 193p.
29. *State Control of Water Quality. Handbook of the Technical Committee for Standardization*, 2nd ed.; IPK Standard Publishing House: Moscow, Russia, 2003; 776p. (In Russian)
30. Wetzel, R.G.; Likens, G.E. *Limnological Analyses*; Springer: New York, NY, USA, 1991; 391p.
31. *Hygienic Norms HN 2.1.5.1315-03—Maximal Permissible Concentration of Chemical Substances in water of the Water Sources of Drinking and Communal Use*; Ministry of Health: Moscow, Russia, 2003; 120p.
32. Khazheeva, Z.I.; Plyusnin, A.M. Current State of Water Resources of Gusinoe Lake (Western Transbaikalia). *Water Resour.* **2018**, *45*, 104–110. [CrossRef]
33. Calmuc, V.; Calmuc, M.; Arseni, C.; Topa, M.; Timofti, L.P.; Georgescu, C.; Iticescu, A. Comparative Approach to a Series of Physico-Chemical Quality Indices used in Assessing Water Quality in the Lower Danube. *Water* **2020**, *12*, 3239. [CrossRef]
34. Calmuc, V.A.; Calmuc, M.; Arseni, M.; Topa, C.M.; Timofti, M.; Burada, A.; Iticescu, C.; Georgescu, L. Assessment of Heavy Metal Pollution Levels in Sediments and of Ecological Risk by Quality Indices, Applying a Case Study: The Lower Danube River, Romania. *Water* **2021**, *13*, 1801. [CrossRef]
35. Shvartsev, S.L.; Zamana, L.V.; Plyusnin, A.M.; Tokarenko, O.G. Equilibrium of nitrogen-rich spring waters of the Baikal Rift Zone with host rock minerals as a basis for determining mechanism of thei formation. *Geochem. Int.* **2015**, *53*, 713–725. [CrossRef]
36. Sklyarov, E.V.; Sklyarova, O.A.; Men'shagin, Y.V.; Danilova, M.A. Mineralized lakes of the Transbaikalia and Northeastern Mongolia: Specific features of occurrence and ore-generating potential. *Geogr. Nat. Resour.* **2011**, *32*, 323–332. [CrossRef]
37. Sklyarova, O.A.; Chudnenko, K.V.; Bychinskiy, V.A. Physico-chemical simulation of the evolution of small lakes in a cold climate. *Geochem. Int.* **2011**, *49*, 827–837. [CrossRef]
38. Borzenko, S.V.; Fedorov, I.A. Some trace elements behavior regularity in mineral lakes of eastern Transbaikalia. *Uspekhi Sovremennogo Estestvoznaniya* **2019**, *1*, 69–74.
39. Sklyarov, E.V.; Sklyarova, O.A.; Men'shagi, Y.V. The concentration of trace elements in small lakes of Chita-Ingoda depression (Eastern Transbaikalia, Russia). *Russ. Geol. Geophys.* **2012**, *53*, 1732–1734.
40. Deberdt, S.; Viers, J.; Dupre, B. New insights about the rare earth elements (REE) mobility in river waters. *Bull. Soc. Geol. Fr.* **2002**, *173*, 147–160. [CrossRef]
41. Pokrovski, O.S.; Schott, J. Iron colloid/organic matter associated transport of major and trace elements in small borest rivers and their estuaries (NW Russia). *Chem. Geol.* **2002**, *190*, 141–181. [CrossRef]
42. Thorslund, J.; Jarsjo, J.; Waldstedt, T.; Mo Carl, M.; Lychagin, M.; Chalov, S. Speciation and hydrological transport of metals in non-acidic river systems of the lake Baikal basin: Field data and model predictions. *Reg. Environ. Chang.* **2017**, *17*, 2007–2021. [CrossRef]
43. Asgari, G.; Rahmani, A.R.; Faradma, J.; Seil Mohammadi, A.M. Kinetic and isotherm of hexavalent chromium adsorption onto nano hydroxyapatite. *Res. Health Sci.* **2012**, *12*, 45–53.
44. Ahmed, I.A.M.; Hamilton-Taylor, J.; Bieroza, M.; Zhang, H.; Davidson, W. Improving and testing geochemical speciation predictions of metal ions in natural waters. *Water Res.* **2014**, *67*, 276–291. [CrossRef]
45. Taylor, S.R.; McLennan, S.M. *The Continental Crust: Its Composition and Evolution*; Blackwell: Oxford, UK, 1985; 312p.
46. Andryushchenko, S.V.; Vorontsov, A.A.; Yarmolyuk, V.V.; Sandimirov, I.V. Evolution of Jurassic-Cretaceous magmatism in the Khambin volcanotectonic complex (Western Transbaikalia). *Russ. Geol. Geophys.* **2010**, *51*, 734–749. [CrossRef]
47. Khubanov, V.B.; Vrublevskaya, T.T.; Tsygankov, A.A.; Vladimirov, A.G.; Buyantuev, M.D.; Sokolova, E.N.; Posokhov, V.F.; Khromova, E.A. Melting conditions of granitoid xenoliths in contact with Alkaline mafic magma (Gusinoozerskaya dyke, Western Transbaikalia): To the problem of the origin of Ultrapotassic acid melts. *Geodyn. Tectonophys.* **2017**, *8*, 347–368. [CrossRef]
48. Khubanov, V.B.; Vrublevskaya, T.T.; Tsyrenova, B.T.; Tsygankov, A.A. Formation of the Trachybasalt–Trachyte Bimodal Series of the Malo_Khamardaban Volcanotectonic Complex, Southwestern Transbaikalia: Role of Fractional Crystallization and Magma Mixing. *Petrology* **2015**, *23*, 451–479. [CrossRef]